INTERNATIONAL JOURNAL FOR NUMERICAL AND ANALYTICAL METHODS IN GEOMECHANICS
Int. J. Numer. Anal. Meth. Geomech., 2006; **30**:615–634
Published online 2 February 2006 in Wiley InterScience (www.interscience.wiley.com). DOI: 10.1002/nag.494

The numerical modelling of advective transport in the presence of fluid pressure transients

A. P. S. Selvadurai*,†,‡ and W. Dong

Department of Civil Engineering and Applied Mechanics, McGill University, 817 Sherbrooke Street West, Montreal, Que., Canada H3A 2K6

SUMMARY

Conventional modelling of transport problems for porous media usually assumes that the Darcy flow velocities are steady. In certain practical situations, the flow velocity can exhibit time-dependency, either due to the transient character of the flow process or time dependency in the boundary conditions associated with potential flow. In this paper, we consider certain one- and three-dimensional problems of the advective transport of a chemical species in a fluid-saturated porous region. In particular, the advective flow velocity is governed by the piezo-conduction equation that takes into account the compressibilities of the pore fluid and the porous skeleton. Time- and/or mesh-refining adaptive schemes used in the computational modelling are developed on the basis of a Fourier analysis, which can lead to accurate and optimal solutions for the advective transport problem with time- and space-dependent advective flow velocity distributions. Copyright © 2006 John Wiley & Sons, Ltd.

KEY WORDS: advective transport; piezo-conduction equation; stabilized numerical methods; time- and mesh-adaptive schemes; transport from cavities

1. INTRODUCTION

The problem that deals with the movement of hazardous chemicals and other contaminants in fluid-saturated porous media is of considerable importance to geoenvironmental engineering [1–6]. The assessment of the distribution of the concentration of a chemical or a contaminant within the porous medium influences the environmental decision-making process. It is rarely possible to conduct large-scale experiments to determine the location of contaminant plumes within the geosphere. In the event of either an accidental chemical spill or a geological disposal of the chemical, recourse must be made to a plausible model to establish the spatial and temporal distribution of the chemical. Even such theoretical approaches are only approximations of very complex transport processes that are influenced by the chemical interaction

*Correspondence to: A. P. S. Selvadurai, Department of Civil Engineering and Applied Mechanics, McGill University, 817 Sherbrooke Street West, Montreal, Que., Canada H3A 2K6.
†E-mail: patrick.selvadurai@mcgill.ca
‡William Scott Professor and James McGill Professor

Received 28 August 2005
Revised 4 October 2005
Accepted 4 October 2005

between the porous medium and the chemical species that is being transported. Purely advective transport is perhaps the simplest approach to the modelling of the movement of a contaminant of a chemical species in the porous medium that can provide useful first approximations of engineering value. The absence of both diffusion effects and natural attenuation can lead to the estimation of the location of contaminant plumes with the strongest concentration, which can then be used to assess the most adverse effects.

In the conventional modelling of the advective transport problem it is invariably assumed that the migration of the contaminant or the chemical species within a fluid-saturated medium is as a result of steady Darcy flow applicable to an incompressible fluid. With geological media such as soils, this is a relevant approximation, particularly when considering the incompressible nature of the pore fluid with respect to the compressibilities of most porous soil fabrics. Selvadurai [7–9] developed analytical solutions to examine the problem of contaminant migration resulting from steady Darcy flow in two- and three-dimensional porous fluid-saturated geological regions. Time dependency in the Darcy flow velocity can exist purely as a result of the time-dependent variation in the boundary potential initiating flow [10]. A further class of time-dependent velocity fields can be introduced to the advective transport problem as a result of the compressibilities of the pore fluid and/or the skeleton of the porous medium. Such compressibility is particularly important when considering the process of advective transport of chemicals through highly porous geological media where the compressibility of the porous skeleton can be comparable to that of the pore fluid. In a complete treatment of the chemical transport problem in such geologic media, the flow velocities will be determined by partial differential equations (PDEs) governing coupled processes for the deformations of the porous medium and pore fluid flow developed by Biot [11] (see also Reference [12]). This paper utilizes a simplified treatment of the coupled behaviour between the deformations of the pore fluid and the porous medium that is restricted to predominantly volumetric deformations of the materials. In such cases, the fluid pressure initiating Darcy flow in the porous medium can be described by the 'Piezo-Conduction' equation [13,14].

The objective of this paper is to examine the advective transport of a chemical species in a fluid-saturated porous medium where the flow velocities are derived from the solution of the piezo-conduction equation. It is implicitly assumed that the chemical that is being transported induces no changes to either the compressibility characteristics of the pore fluid or the hydraulic characteristics of the porous medium. The paper presents a computational approach to the solution of the weakly coupled system of PDEs and discusses a *novel* time- and/or mesh-refining adaptive numerical scheme that can satisfactorily address advective transport problems where the leading edge of the migration front has a sharp discontinuity. In particular, certain three-dimensional problems involving migration from a pressurized crack are discussed.

2. GOVERNING EQUATIONS

The generalized problem of the advective transport of a chemical species in a fluid-saturated porous medium is governed by the following PDE for the scalar concentration of the chemical $C(\mathbf{x}, t)$

$$\frac{\partial C}{\partial t} + \mathbf{v}\nabla C + C\nabla \cdot \mathbf{v} = 0 \tag{1}$$

where $\mathbf{x}$ is a position vector, t is time, $\mathbf{v}(\mathbf{x}, t)$ is the averaged advective flow velocity in the pore space. The third term on the LHS of (1) is non-zero if the fluid is considered to be compressible. The advective flow velocity in the porous medium is assumed to be governed by Darcy's law, which for an isotropic porous medium can be expressed by

$$\mathbf{v} = -k\nabla\phi \tag{2}$$

In (2), k is the Dupuit–Forchheimer hydraulic conductivity which is related to the conventional area averaged hydraulic conductivity $\tilde{k}$ by the relation $k = \tilde{k}/n^*$ and n^* is the porosity, $\phi(\mathbf{x}, t)$ is the flow potential inducing flow, which consists of the datum potential ϕ_D and the pressure potential ϕ_p, i.e. $\phi = \phi_D + \phi_p$. Considering the compressibilities of the pore fluid and the porous skeleton as well as the mass conservation during the flow, the PDE governing the advective flow potential can be reduced to the classical piezo-conduction equation

$$D_p\nabla^2\phi_p = \frac{\partial\phi_p}{\partial t} \tag{3}$$

This reduction assumes that the pressure potential is much higher than the datum potential. The pressure diffusion coefficient D_p in (3) is given by

$$D_p = \frac{k}{\gamma_w[n^*C_f + C_s]} \tag{4}$$

where C_f and C_s are the compressibilities of the pore fluid and the porous skeleton, respectively, and γ_w is the unit weight of water. In the sense that the flow velocity field is uninfluenced by the chemical transport process, the governing PDEs (1) and (3) can be regarded as being weakly coupled.

3. NUMERICAL SCHEMES

3.1. Stabilized semi-discrete Eulerian methods

Conventional computational schemes perform poorly in solving advection-dominated problems that have a purely hyperbolic character. They introduce either oscillations or artificial diffusion in the vicinity of discontinuous concentration profiles. To date, many stabilized finite element methods have been developed for the accurate solution of the advection equation with the solution containing a discontinuity (see e.g. References [15,16]). The basic concept underlying these stabilized methods is to introduce, with the aid of asymmetric weighting functions, artificial diffusion in the vicinity of a steep front of the solution. In this approach, a perturbation is introduced into the conventional Galerkin weighting function, which should be added to the 'flow' direction to avoid crosswind diffusion [17]. The general residual integral form of the stabilized semi-discrete Eulerian method for the advection equation over domain V has the following form [18]:

$$\int_V \left[w + \alpha_1 \frac{\mathbf{v}}{\|\mathbf{v}\|}\cdot\nabla w\right]\frac{\partial C}{\partial t}\,\mathrm{d}V + \int_V \left[w + \alpha_2 \frac{\mathbf{v}}{\|\mathbf{v}\|}\cdot\nabla w\right](\mathbf{v}\nabla C^{n+\theta})\,\mathrm{d}V = 0 \tag{5}$$

where w is the standard Galerkin weighting function. In (5), α_i $(i = 1, 2)$ are perturbation parameters referred to as the upwind functions or the intrinsic times of the stabilized methods [19]. They can be determined using a least squares (LS) method [20], such that the artificial

convection term has the adjoint form of the advection term in the equation, which gives rise to computational schemes that are symmetric [21]. Alternatively, their choice can be based on a Fourier analysis to ensure that numerical modelling gives rise to an 'optimal' solution of the transient advection equation [22], such as the one in streamline upwind Petrov–Galerkin method proposed by Hughes and Brooks [17]. The upwind function can also take different values to generate different stabilized methods, such as the Taylor–Galerkin method [23].

3.2. The modified LS method

Since the LS method can generate a symmetric matrix form for the advection equation, the method has significant potential for the examination of the non-linear problem. Wendland and Schmid [21] proposed the 3S scheme (Symmetrical Streamline Stabilization) for the numerical modelling of the advection-dominated transport problem, in which a parameter was introduced into the upwind term of the LS scheme to obtain optimal computational performance. This approach is equivalent to using different perturbation parameters in the weighting functions for the temporal and spatial terms of the advection equation in the LS method: i.e.

$$\int_V [w + \theta \Delta t \mathbf{v} \cdot \nabla w] \frac{\partial C}{\partial t} \, \mathrm{d}V + \int_V [w + \alpha \theta \Delta t \mathbf{v} \cdot \nabla w](\mathbf{v} \cdot \nabla C^{n+\theta}) \, \mathrm{d}V = 0 \tag{6}$$

and therefore this scheme can be referred to as the modified LS (MLS) method. The parameter α in (6) accounts for the upwind effect, which can be determined from a Fourier analysis to achieve a better numerical performance of the MLS scheme for the advection equation.

4. TIME- AND SPACE-ADAPTIVE PROCEDURES

4.1. Fourier analysis

The mathematical performance of stabilized semi-discrete Eulerian methods for the advection equation can be demonstrated via a Fourier analysis in the frequency domain by means of the algorithmic amplitude and the phase velocity of the numerical scheme [24, 25]. Selvadurai and Dong [26] performed a Fourier analysis of the MLS scheme for the advection equation and obtained the following analytical expressions for the algorithmic amplitude ζ^h and the relative phase velocity u^*/u of the MLS method applicable for the one-dimensional advection equation with the application of the trapezoidal rule

$$\zeta^h = |z(\omega)| = \frac{\sqrt{[2 + \cos(\omega h) - 6\alpha Cr^2\theta(1-\theta)(1-\cos(\omega h))]^2 + 9Cr^2 \sin^2(\omega h)}}{2 + \cos(\omega h) + 6\alpha Cr^2\theta^2(1-\cos(\omega h))} \tag{7a}$$

$$\frac{u^*}{u} = \frac{\Omega^h}{\omega} = -\frac{\arg(z(\omega))}{\omega \Delta t} = \frac{1}{Cr\omega h} \arctan\left(\frac{3Cr \sin(\omega h)}{2 + \cos(\omega h) - 6\alpha Cr^2\theta(1-\theta)(1-\cos(\omega h))}\right) \tag{7b}$$

where $z(\omega)$ is the spectral function of the MLS numerical operator for the advection equation with the application of the trapezoidal rule, Cr $(= u\Delta t/h)$ is the Courant number, u is the one-dimensional flow velocity, h is the length of the piecewise element, ωh is dimensionless wave

number and θ is time weighting. From the analytical expression (7), the following results can be obtained for the optimal values of the algorithmic amplitude and the relative phase velocity of the MLS scheme for the advection equation

$$\zeta^h\big|_{\alpha=3/2,\theta=1/3,Cr=1} = 1 \tag{8a}$$

$$\left.\frac{u^*}{u}\right|_{\alpha=3/2,\theta=1/3,Cr=1} = 1 \tag{8b}$$

Figure 1 shows the variation of the algorithmic amplitude and the phase velocity given by (7) with the definition of $\alpha = 3/2$ and $\theta = 1/3$ with the Courant number Cr and the dimensionless wave number ωh.

4.2. Courant number criterion

The results (8) imply that with $\alpha = 3/2$, $\theta = 1/3$ and $Cr = 1$, there are no errors in the algorithmic amplitude and the phase velocity of the MLS scheme for the advection equation for all values of the dimensionless wave number ωh, and therefore all wave components included in the solution will travel at the same speed without shape distortion. This indicates that the MLS method with $\alpha = 3/2$ and $\theta = 1/3$ can generate an accurate solution for the advection equation under the condition of $Cr = 1$. Such optimal conditions for the MLS scheme can be used in conjunction with the time- and/or mesh-adaptive procedures to obtain an accurate solution for the advective transport problem characterized particularly by a discontinuous leading edge and initiated by a time- and space-dependent flow field. In such time- and/or mesh-adaptive schemes, the time step Δt, or elemental length h_{ie} of the elements in regions where a steep front of the solution is plausibly located, should be determined on the basis of the Courant number criterion

$$(Cr)_{ie} = \frac{\|\mathbf{v}\|_{ie}\Delta t}{h_{ie}} = 1 \tag{9}$$

where ie refers to the elements where the steep front is located, h_{ie} and $\|\mathbf{v}\|_{ie}$ are, respectively, the characteristic length and magnitude of the flow velocity within the element ie. The steep front of

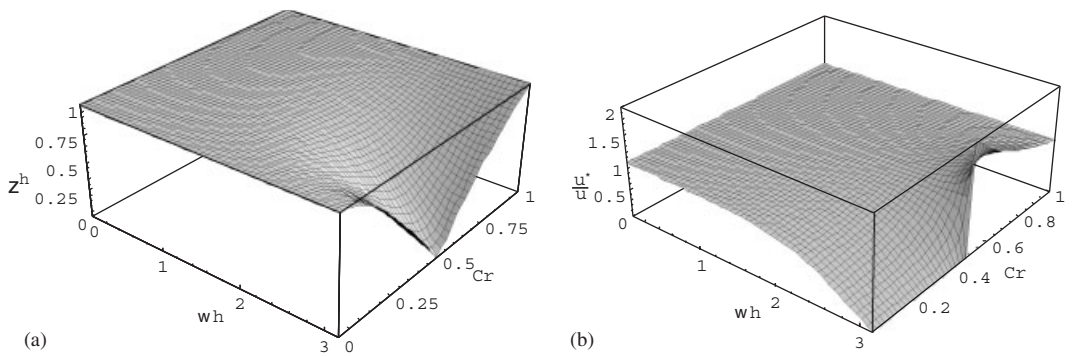

Figure 1. The variation of: (a) the algorithmic amplitude; and (b) the relative phase velocity of the MLS scheme with $\alpha = 3/2$ and $\theta = 1/3$ for the advection equation with Cr and ωh.

the solution is located through an error indicator $E(e)$, based on the first derivative of the solution for each element [27]

$$E(e) = \left(\frac{1}{2} \cdot \sum_{j \in \partial e} h_j^2 [\mathbf{n}_j \cdot \nabla C]^2 \right)^2 \tag{10}$$

where $\mathbf{n}_j$ is the unit normal to the edge j of the element with the length h_j and ∂e is the boundary of the element. The term in square brackets in (10) represents the jump in the flux across the element edge. The locations (or elements) of the steep front are determined by satisfying $E(e) > \beta$ and β is a parameter, which can be defined by the half of the maximum of $E(e)$, i.e. $\beta = 0.5 \ \max(E(e))$.

In the ensuing sections, the time- and mesh-adaptive procedures will be used in conjunction with the MLS scheme to examine the advective transport problems associated with one- and three-dimensional axisymmetric configurations where the advective flow velocities are both time- and space-dependent and derived from the transient pressure potential governed by the piezo-conduction equation (3).

5. A ONE-DIMENSIONAL ADVECTIVE TRANSPORT PROBLEM

5.1. The transport equation with the analytical transient flow velocity

In this section, a one-dimensional problem of the advective transport of a chemical species in a fluid-saturated porous medium is examined. The advective flow velocity is determined by the flow potential, which is governed by the following initial boundary value problem (IBVP) applicable to a one-dimensional semi-infinite region: the governing PDE is

$$D_p \frac{\partial^2 \phi_p}{\partial x^2} = \frac{\partial \phi_p}{\partial t} \tag{11a}$$

and the boundary and regularity conditions and initial conditions are, respectively,

$$\phi_p(0, t) = \phi_0 H(t), \quad \phi_p(\infty, t) \to 0 \tag{11b}$$

$$\phi_p(x, 0) = 0, \quad x \in [0, \infty) \tag{11c}$$

where $H(t)$ is the Heaviside step function. An analytical solution for the IBVP (11) has the following form (see e.g. References [6, 28]:

$$\phi_p(x, t) = \phi_0 \ \mathrm{erfc}\left(\frac{x}{2\sqrt{D_p t}} \right) \tag{12}$$

where $\mathrm{erfc}(x)$ is the complimentary error function defined by

$$\mathrm{erfc}(x) = 1 - \frac{2}{\sqrt{\pi}} \int_0^x \mathrm{e}^{-\xi^2} \, \mathrm{d}\xi \tag{13}$$

From (12), the flow velocity in the semi-infinite porous region is given by

$$v(x,t) = -k\frac{\partial \phi_p}{\partial x} = k\phi_0\left(\frac{1}{\sqrt{\pi D_p t}}\,\exp\left(-\frac{x^2}{4D_p t}\right)\right) \tag{14}$$

Therefore, the one-dimensional problem of advective transport in the semi-infinite porous region is governed by the following PDE:

$$\frac{\partial C}{\partial t} + k\phi_0\left(\frac{\exp(-x^2/4D_p t)}{\sqrt{\pi D_p t}}\right)\frac{\partial C}{\partial x} - k\phi_0\left(\frac{x\,\exp(-x^2/4D_p t)}{2\sqrt{\pi}(D_p t)^{3/2}}\right)C = 0 \tag{15}$$

The solution of (15) is subject, respectively, to the following initial and boundary conditions:

$$C(x,0) = 0, \quad x \in [0,\infty) \tag{16a}$$

$$C(0,t) = C_0 H(t) \tag{16b}$$

The IBVP defined by (15) and (16) is well-posed. In the computational modelling of the problem, however, we assume that the concentration profile will satisfy a physically consistent regularity condition

$$C(x,t) \to 0 \quad \text{as } x \to \infty \tag{17}$$

5.2. *Computational modelling*

For the purpose of the computational modelling, we restrict attention to the following specific problem where a constant flow potential $\phi_0 = 100$ m is applied at the upstream boundary. The Dupuit–Forchheimer hydraulic conductivity and the porosity of the porous medium are chosen as $k = 0.03$ m/day and $n^* = 0.3$, respectively, the compressibilities of the porous aquifer material and the pore fluid are taken as $C_s = 1.0 \times 10^{-8}$ m^2/N and $C_f = 4.4 \times 10^{-10}$ m^2/N, respectively. For the fluid-porous medium combination, the specific storage is approximately equal to $S_s = 1.0 \times 10^{-8}$ m^2/N. The transport process is simulated by a finite element model applicable to a domain of finite extent, $V = [0, l]$ with $l = 30$ m. In view of the truncation of the infinite domain and in the absence of the use of appropriate infinite elements, the regularity condition in (11b) is replaced by the Neumann boundary condition applicable at the downstream boundary, i.e. $[\partial C/\partial x]\big|_{x=l} = 0$. The computational domain V is discretized into 300 piecewise linear elements with identical length $h = 0.1$ m. The distribution of the flow potential and the flow velocity over the finite domain, obtained from analytical solutions (12) and (14), respectively, during a period of 10 days are shown in Figure 2. It is evident that the flow velocity has a strong time- and space-dependency due to the presence of pressure transients.

In order to validate the necessity and the efficiency of the computational scheme involving the time-adaptive procedure, we shall first examine the numerical results for the advective transport problem derived from the MLS scheme both with and without the time-adaptive procedures. In the time-adaptive procedure, the time step during the computation is determined by the Courant number criterion (9) and by the magnitude of the flow velocity in the element where the steep front of the solution is located. Figure 3 illustrates the corresponding numerical results determined from the two approaches for the advective transport process governed by (15). These results clearly indicate that in the absence of a time-adaptive procedure, the MLS method generates oscillations in the solution, due to the spatial and temporal variations in the flow

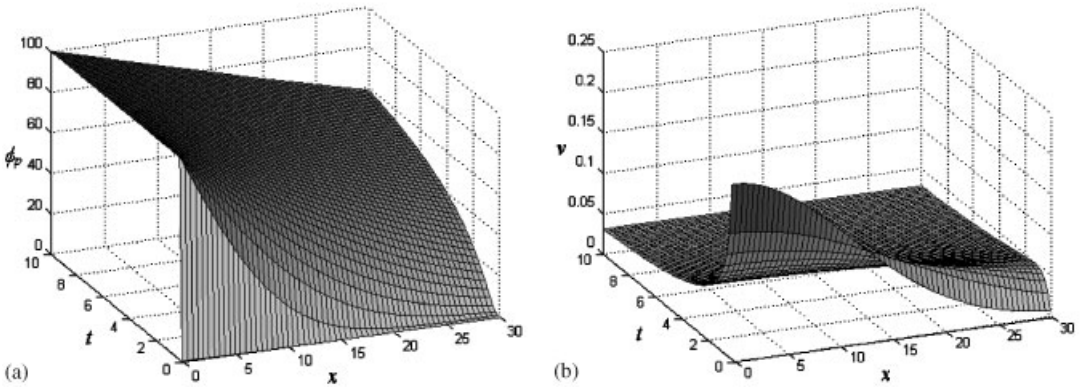

Figure 2. The distribution of: (a) the flow potential; and (b) the flow velocity in the time–space region.

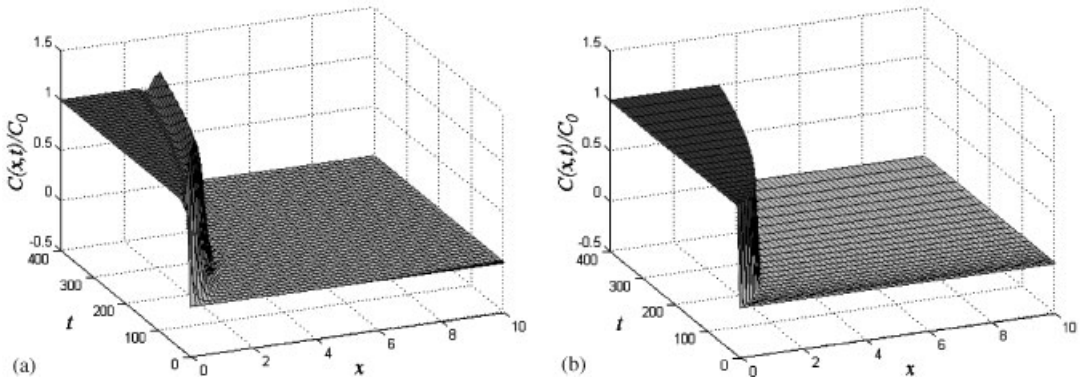

Figure 3. Computational results corresponding to $t = 400$ days for the advective transport with a transient advective flow velocity in a porous region obtained from the MLS method: (a) without time-adaptive procedure; and (b) with time-adaptive procedure.

velocity; the time-adaptive MLS scheme, on the other hand, gives oscillation-free and non-diffusive computational results for the concentration profile resulting from one-dimensional advective transport with transient flow velocities. In the computational scheme associated with the time-adaptive technique, the initial time step of $\Delta t = 0.2$ days finally increases to $\Delta t = 33$ days to satisfy constraint (9) imposed by the Courant number criterion.

6. THREE-DIMENSIONAL AXISYMMETRIC ADVECTIVE TRANSPORT PROBLEMS

Next, we focus attention on a problem involving advective transport of a chemical from a flattened cavity in a porous medium (Figure 4). This problem is of practical importance in connection with the deep geological disposal of hazardous chemicals in a hydraulically fractured cavity at the base of a borehole. Since the problem is axisymmetric and the geometry of the

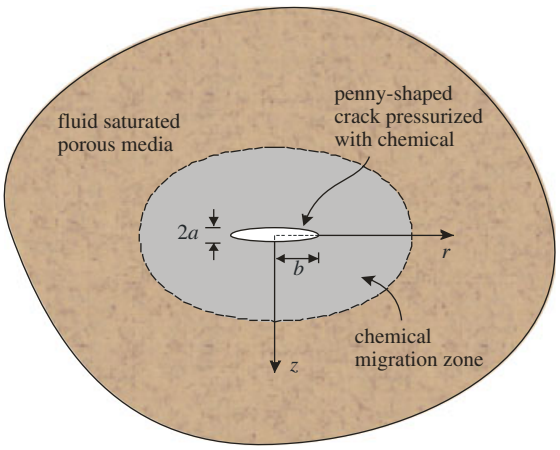

Figure 4. A concept for deep geological disposal of hazardous chemicals.

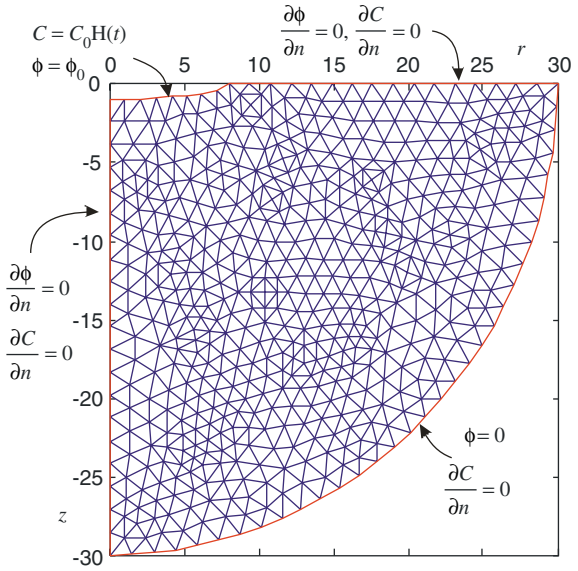

Figure 5. The finite element discretization of the computational domain and the associated boundary conditions for the flow and the advective transport from an oblate spheroidal cavity.

cavity also exhibits symmetry about the plane $z = 0$, attention can be restricted to the consideration of a quarter-domain where suitable Neumann boundary conditions are imposed to satisfy requirements of symmetry. The boundary conditions corresponding to a cavity region with $a = 8$ m and $b = 1$ m are shown in Figure 5. The outer boundary is fixed at a radius $R(= \sqrt{r^2 + z^2}) = 30$ m where a Neumann boundary condition is applied to $C(\mathbf{x}, t)$ in order to achieve the required regularity condition at infinity. The Dupuit–Forchheimer measure of hydraulic conductivity of the porous medium is taken as $k = 0.03$ m/day. The boundary of the

cavity is subject to a potential $\phi_0 H(t)$ and the far field potential is maintained at a zero value as shown in Figure 5.

6.1. Mesh-refining adaptive scheme

The computations presented in Section 5 indicate that the MLS scheme with the chosen values of $\alpha = 3/2$ and $\theta = 1/3$ can generate an accurate solution for the advection equation when the elemental Courant number is kept at unity in regions where the steep front of the solution is located. From the basis for the observation presented in Section 4, it is noted that the accuracy of the solution obtained from the MLS scheme for the advection equation is sensitive to the Courant number criterion (9). For one-dimensional problem, it is relatively easy to satisfy the Courant number criterion by selecting the time step based on the time-adaptive procedure. When dealing with spatially multi-dimensional transport problems, especially with finite element discretizations that use elements of arbitrary shape and size, it is difficult to choose a single time step for which the Courant number criterion (9) is satisfied by all elements with different magnitudes of flow velocities and characteristic lengths, particularly at the leading edge of a discontinuous concentration front. Once the Courant number exceeds unity, the MLS scheme with $\alpha = 3/2$ and $\theta = 1/3$ will become unstable since $\zeta^h > 1$. Therefore conservative values of α, θ and Cr should be used to ensure that the scheme is always stable, i.e. $\zeta^h \leqslant 1$. This implies that the requirement $\zeta^h \equiv 1$ imposed by the Courant number criterion may not be exactly satisfied. The conservative choices of α and θ should be determined from the consideration of the following aspects: (i) since $\zeta^h \equiv 1$ may not be satisfied, the condition $u^*/u \equiv 1$ must be satisfied; (ii) since there is only one remaining equation, one of two parameters α and θ can be determined beforehand, and usually the time weighting θ is chosen as $\theta = 1/2$ such that the scheme has a greater accuracy in the time-integration scheme (i.e. the Crank–Nicholson (CN) time integration scheme). Substituting $\theta = 1/2$ into (7b) leads to the following results for the phase velocity of the MLS scheme for the advection equation:

$$\left.\frac{u^*}{u}\right|_{\alpha=4/3,\theta=1/2,Cr=1} \equiv 1 \tag{18a}$$

$$\left.\frac{u^*}{u}\right|_{\alpha=4/3,\theta=1/2,Cr=1/2} \equiv 1 \tag{18b}$$

From (18), we observe that by specifying $\alpha = 4/3$ and $\theta = 1/2$, no error will occur in the phase velocity of the CN-MLS scheme (CN-MLS) when $Cr = 1/2$ and $Cr = 1$. Figure 6 illustrates the variation in the algorithmic amplitude ζ^h and relative phase velocity u^*/u of the CN-MLS scheme with the Courant number $Cr \in [0, 3]$ and the dimensionless wave number $\omega h \in [0, \pi]$. From the variations shown in Figure 6 it is evident that although (18a) and (18b) are satisfied, ζ^h will decay much faster when $Cr = 1/2$ than when $Cr = 1$. This observation indicates that the CN-MLS scheme is more diffusive for $Cr = 1/2$ than for $Cr = 1$, and an adaptive procedure that is based on Courant number criterion (9) should also be combined with the CN-MLS scheme to obtain better numerical performance in the case of multi-dimensional advective transport problems.

With the Courant number criterion (9), the h-refinement of a mesh-adaptive algorithm [29, 30] can be developed with the CN-MLS scheme to obtain an optimal numerical solution for the advective transport problem governed by a time- and space-dependent flow velocity field. In

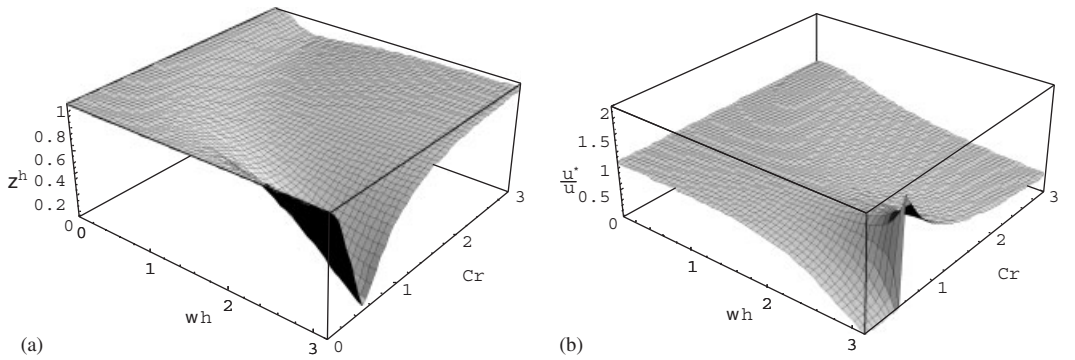

Figure 6. The variation of: (a) the algorithmic amplitude; and (b) the relative phase velocity of the MLS scheme with $\alpha = 4/3$ and $\theta = 1/2$ for the advection equation with Cr and ωh.

such a mesh-adaptive scheme, the mesh at the locations of the steep front of the solution can be refined quantitatively with the Courant number criterion (9) based on the magnitude of the flow velocity. Since the size of the element will be decreased during the mesh refinement, the elemental Courant number will be increased. Therefore, in order to avoid high elemental Courant numbers, the criterion $(Cr)_{ie} \leqslant 0.5$ should be used in the mesh-adaptive algorithm, such that the Courant numbers in the refined elements do not exceed unity. In such a mesh-refining approach, only the elements where the high gradient of the solution is encountered need be refined by reducing the dimensions of all the edges or the longest edge of the selected triangles into half their original length. This mesh-refining adaptive scheme will be used in the ensuing section to develop computational results for the advective transport of a contaminant from the boundary of an oblate spheroidal cavity, induced by both steady flow and unsteady flow.

6.2. The advective transport with a steady fluid flow

First, the steady-state problem of the advective transport from the oblate spheroidal cavity in a non-deformable porous medium is considered (i.e. the pore fluid is considered to be incompressible and the porous skeleton is assumed to be non-deformable). In this case, the piezo-conduction equation reduces to Laplace's equation, and the corresponding steady flow velocity field resulting from the flow potential boundary conditions indicated in Figure 5 is shown in Figure 7. The results indicate that the flow velocity field has a strong spatial dependency and decays rapidly for points located remote from the pressurized cavity. Selvadurai [10] gave an exact closed-form analytical solution for the advective transport from the oblate spheroidal cavity when a steady flow is induced in the porous domain of infinite extent through the application of a constant potential at the cavity boundary. Figure 8 shows the analytical solution at time $t = 30$ days, applicable to a quarter of the domain shown in the Figure 4. The corresponding computational results shown in Figure 9 were obtained from the CN-MLS scheme without the application of the adaptive procedure. In the numerical computations, the time step is chosen as $\Delta t = 1.0$ day such that the elemental Courant number near the cavity boundary is approximately equal to the optimum value of unity. It can be noted that numerical oscillations are introduced into the solution in the vicinity of the steep edge

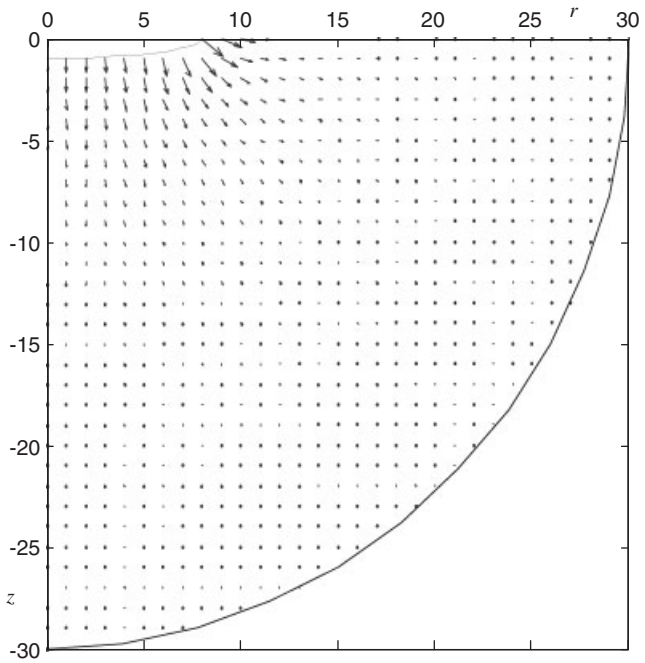

Figure 7. The flow velocity pattern in the computational domain containing an oblate cavity.

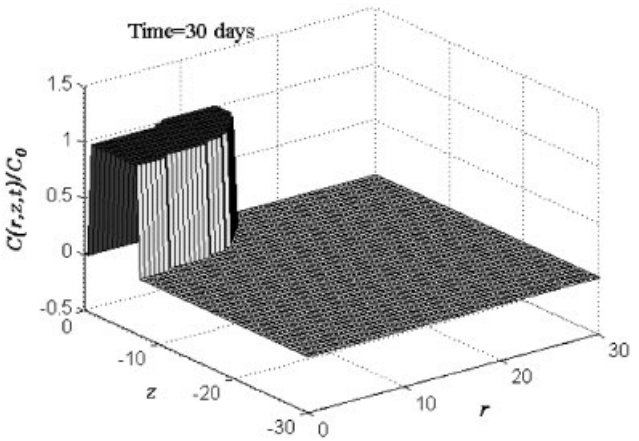

Figure 8. The analytical solution of the advective transport from an oblate spheroidal cavity ($a/b = 0.125$) [10].

located remote from the cavity, due to the small magnitude of the flow velocity, which induces the low Courant number and the large discrepancy between the phase velocity and the flow velocity. If the time step is increased, the numerical oscillations will be introduced into the solution at the early stages of the transport process (i.e. the steep front is located in the vicinity

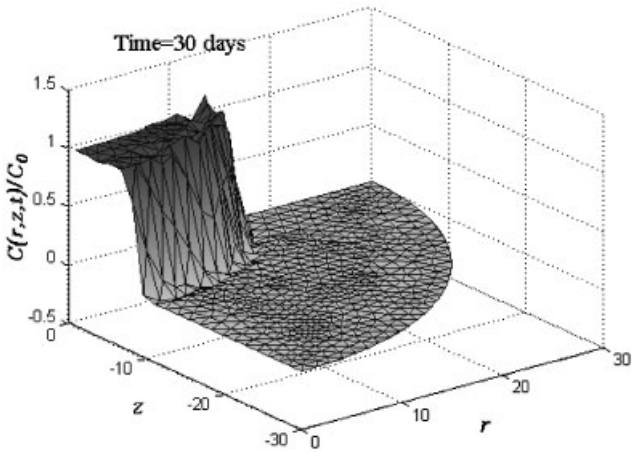

Figure 9. Numerical results at $t = 30$ days for the advective transport from the oblate cavity obtained from the CN-MLS scheme with $\Delta t = 1.0$ days.

of the cavity) due to the high Courant number resulting from the large magnitude of the flow velocity. In the transport processes where the flow field exhibits spatial variations of the type indicated in Figure 7, it is difficult to choose a constant time step with an almost uniform mesh (similar to that shown in Figure 5) to ensure that the elemental Courant number is unity over the entire computational domain. For this reason, adaptive procedures should be used during the computations to satisfy the Courant number criterion (9) at all times. This conclusion can be verified through a numerical computation obtained from a time-adaptive scheme.

The application of the time-adaptive procedure is based on the consideration that the advective flow field along the steep front of the solution is almost uniformly distributed (see Figure 7) and that the element sizes are approximately the same (see Figure 5). In such a time-adaptive procedure, the time step is determined by satisfying the criterion (9), which takes the form

$$\Delta t = \min_{ie} \left(\frac{h_{ie}}{\|\mathbf{v}\|_{ie}} \right) \tag{19}$$

The minimum value of (19) ensures that the time step selected maintains the elemental Courant number along the steep front to a value less than unity. Figure 10 illustrates the numerical results obtained from such a time-adaptive CN-MLS scheme, from which it is noted that serious oscillations introduced by the CN-MLS scheme (without the time-adaptive procedure) are eliminated due to the appropriate choice of the time step. Since the magnitude of the flow velocity is relatively large in regions where the transport process commences, the time step should be kept small to satisfy (19), and should subsequently be increased due to the reduction in the magnitude of the flow velocity when the steep front migrates to a remote region where the flow velocities are comparatively smaller. Using this procedure, the initial time step of $\Delta t = 1$ day increases to $\Delta t = 7.6$ days at the termination of the computation process.

Since arbitrary triangular elements are used in the computational modelling and the time step determined by (19) is a minimum, the Courant number in certain elements where the steep front

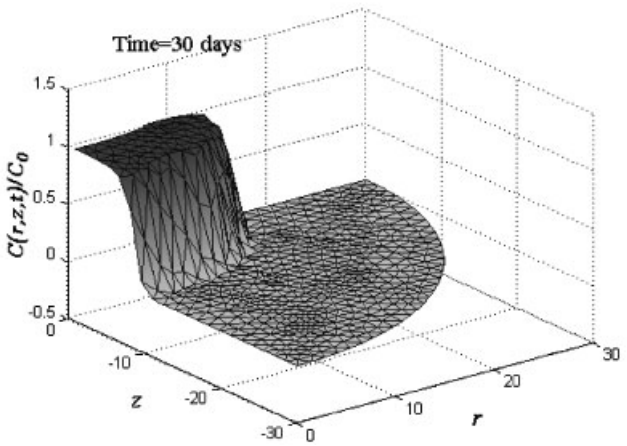

Figure 10. Numerical results at $t = 30$ days for the advective transport from the oblate cavity obtained from the time-adaptive CN-MLS scheme (the initial time step $\Delta t = 1.0$ days is increased to $\Delta t = 7.6$ days).

is located may not be close to the optimum value of unity. This discrepancy will lead to small oscillations in the concentration profile, which are illustrated in Figure 10. Furthermore, the numerical scheme also has an over-diffusive character due to the decay of the algorithmic amplitude for high wave numbers corresponding to $Cr = 1.0$ (see Figure 6(a)). A way of avoiding this over-diffusive feature in the solution is through a reduction of the element size, rather than through an increase of the time step based on Courant number criterion (9). Reducing the element size is equivalent to lowering the dimensionless wave number ωh, thereby compensating for the decay in the algorithmic amplitude of the scheme for high ωh.

Figure 11 shows the numerical solutions obtained from the CN-MLS scheme combined with the mesh-refining adaptive procedure just described. These computational results indicate that the mesh-refining adaptive CN-MLS scheme can generate satisfactory numerical estimates for the linear advective transport in multi-dimensional domains. The effect of the numerical diffusion embedded in the CN-MLS scheme (see discussion in the previous section) is also presented in these numerical results, but it is much smaller than that introduced by the time-adaptive scheme. Judging from the flow pattern shown in Figure 7 and the Courant number criterion (9), it should be noted that the elements located remote from the cavity should be subjected to greater refinement than those located in the vicinity of the cavity. The mesh-refining attributes of the computational scheme are shown in Figure 11. With the mesh-refining adaptive procedure, the MLS scheme with $\alpha = 3/2$ and $\theta = 1/3$ is also considered in modelling the advective transport problem from the oblate spheroidal cavity and the corresponding numerical results are shown in Figure 12. The results in Figure 12 also indicate that serious oscillations are introduced into the solution by the numerical scheme even with the use of the mesh-adaptive procedure, due to the instability of the scheme caused by the inappropriate choice of the Courant number.

The time-adaptive procedure can be combined with the mesh-refining adaptive scheme to improve the efficiency of the computational approach. Figure 13 illustrates the corresponding numerical solution obtained using both the time- and mesh-adaptive schemes. The initial time

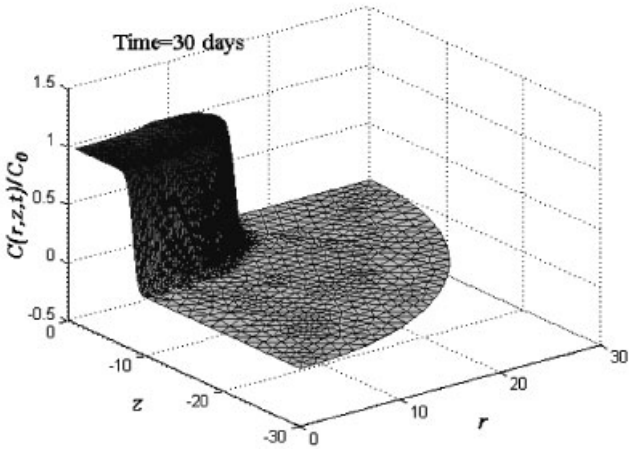

Figure 11. Numerical results at $t = 30$ days for the advective transport from the oblate cavity obtained from the mesh-adaptive CN-MLS scheme with $\Delta t = 1.0$ days.

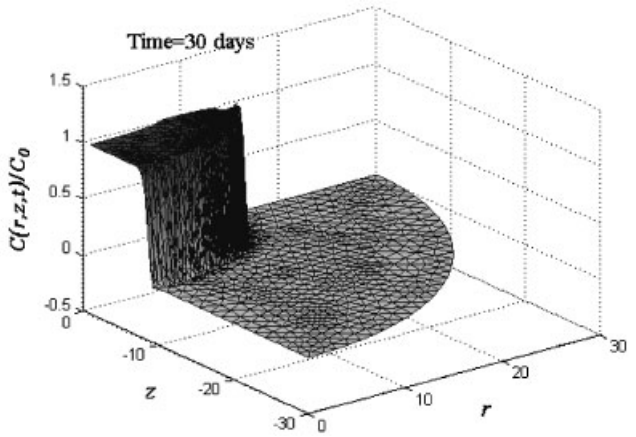

Figure 12. Numerical results at $t = 30$ days for the advective transport from the oblate cavity obtained from the mesh-adaptive MLS scheme with $\alpha = 3/2$ and $\theta = 1/3$.

step of $\Delta t = 1.0$ day adaptively increases to $\Delta t = 5.5$ days at the end of the computation. With the increase in the time step, the mesh refinement is performed on a coarser level than that used in the mesh-adaptive scheme. From this point of view, the combined time- and mesh-adaptive scheme is computationally more efficient than the purely mesh-adaptive scheme. However, because of the use of the coarser refined mesh, the numerical solution obtained from the combined time- and mesh-adaptive scheme is more diffusive than that obtained from the mesh-adaptive scheme.

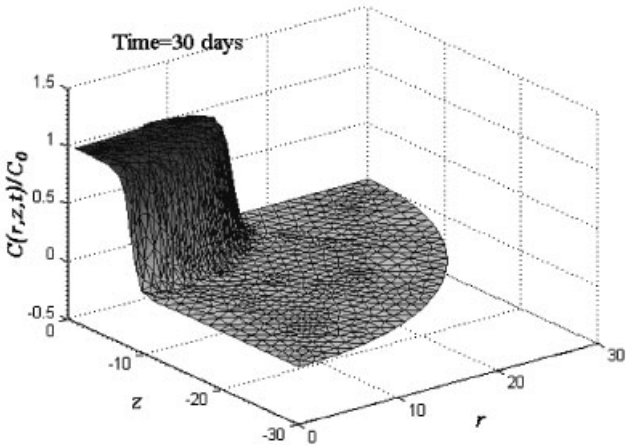

Figure 13. Numerical results at $t = 30$ days for the advective transport from the oblate cavity obtained from the time- and mesh-adaptive CN-MLS scheme (the initial time step $\Delta t = 1.0$ days is increased to $\Delta t = 5.5$ days).

6.3. *Advective transport from an oblate spheroidal cavity induced by pressure transients*

In this section, we consider the advective transport problem where the flow velocities are governed by the piezo-conduction equation, which takes into consideration the compressibilities of the pore fluid and the soil skeleton. Attention is focused on the advective transport of a chemical from an oblate spheroidal cavity located in an extended porous medium where the boundary of the cavity is simultaneously subjected to pressure and chemical pulses in the form of Heaviside step function. The material and physical parameters governing hydraulic conductivity, compressibilities and porosity are kept the same as those used in Section 5. The mesh-refining adaptive as well as the combined time- and mesh-refining adaptive CN-MLS schemes are used to solve the pressure transient-induced advective transport problem. Figure 14 illustrates the numerical results obtained from the two adaptive schemes. In the combined time- and mesh-refining adaptive scheme, the initial time step commences with $\Delta t =$ 1.0 day and increases to $\Delta t = 5.5$ days at the end of the computation corresponding to $t = 30$ days. Again, the mesh-adaptive scheme generates a more accurate solution, but the combined time- and mesh-adaptive scheme is considered to be more efficient.

6.4. *Advective transport from a cylindrical cavity*

As a final example, we consider the problem of advective transport from a cylindrical cavity located in an extended porous medium. The chemical is introduced at the boundary of the borehole and its migration through the porous medium is as a result of a time- and space-dependent velocity field. Figure 15(a) illustrates the axisymmetric computational domain and its discretization as well as the boundary conditions applicable to the piezo-conduction equation and the advection equation. Figure 15(b) illustrates the flow field over the computational domain corresponding to $t = 30$ days, which is determined from the piezo-conduction equation and the potential boundary conditions. The computational results and the refined mesh for the advective transport from the borehole corresponding to $t = 30$ days, obtained from the

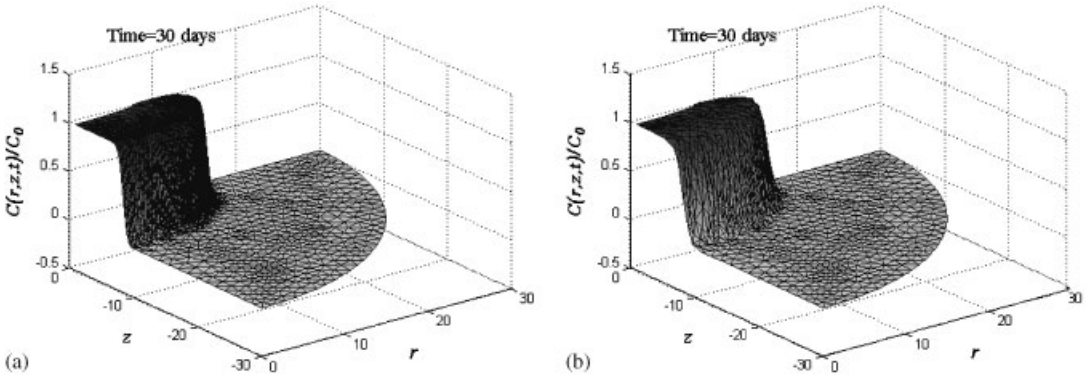

Figure 14. Numerical results at $t = 30$ days for the advective transport from the oblate cavity with pore pressure transient obtained from: (a) the mesh-adaptive CN-MLS scheme; and (b) the combined time- and mesh-refining adaptive CN-MLS scheme (the initial time step $\Delta t = 1.0$ days is increased to $\Delta t = 5.5$ days).

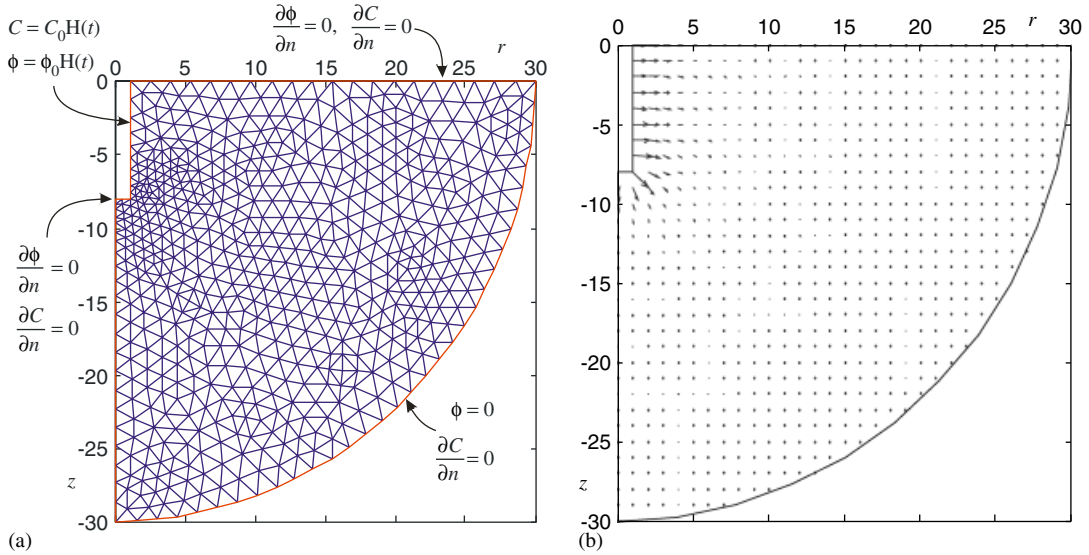

Figure 15. The finite element discretization of the computational domain containing a borehole and the associated boundary conditions: (a) mesh discretization; and (b) flow field at $t = 30$ days.

combined time- and mesh-refining CN-MLS scheme, are shown in Figure 16. In this computation, the initial time step is chosen as $\Delta t = 0.2$ days and it increases to $\Delta t = 7.9$ days as the time-adaptive feature comes into effect.

Finally, we consider the advective transport problem where a time-dependent potential is applied at the boundary of the borehole. This time-dependency in the boundary potential has the form

$$\phi_0 = \begin{cases} 100, & t \leqslant 20 \text{ days} \\ 200, & t > 20 \text{ days} \end{cases} \tag{20}$$

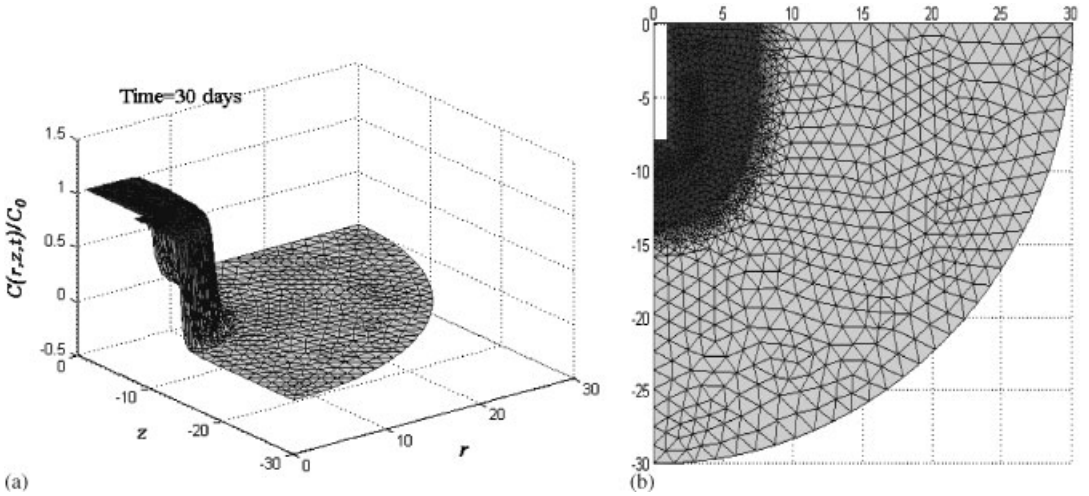

Figure 16. Numerical results for $t = 30$ days for the advective transport from a borehole with pressure transient obtained using a mesh-adaptive CN-MLS scheme: (a) 3D concentration profile; and (b) the corresponding refined mesh.

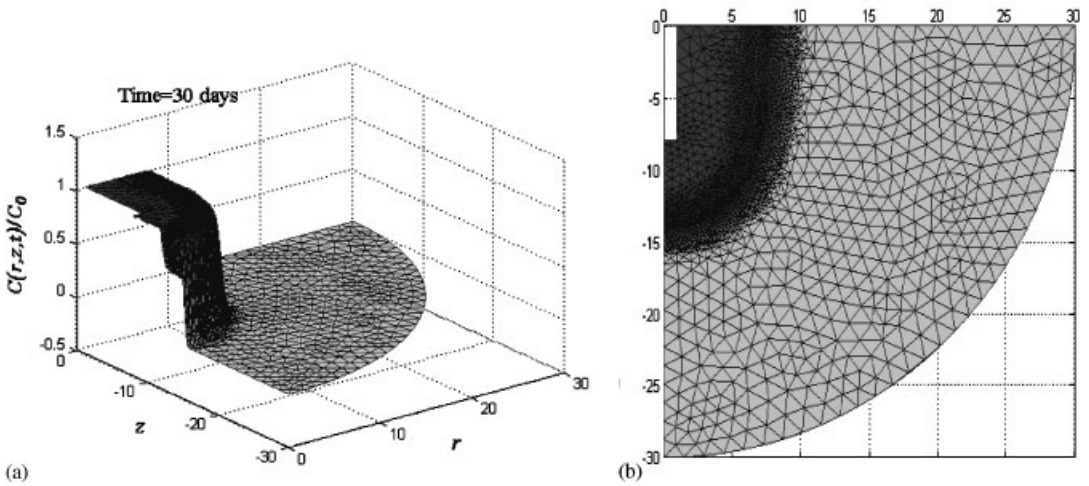

Figure 17. Computational results for $t = 30$ days of the advective transport from a borehole with pulsed potential boundary, obtained using the mesh-adaptive CN-MLS scheme: (a) 3D concentration profile; and (b) the corresponding refined mesh.

The computational results and the refined mesh corresponding to $t = 30$ days, obtained from the mesh-refining CN-MLS scheme with $\Delta t = 1.0$ day, are shown in Figure 17. A mesh gap can be clearly seen in the refined mesh, which corresponds to an increase of the flow velocity caused by a rise in the potential pulse applied at the boundary of the borehole. This increase of the flow velocity has the effect of accelerating the transport process (see e.g. the results shown in Figures 16(a) and 17(a)).

7. CONCLUSIONS

In this paper, certain advective transport problems for fluid-saturated porous media are examined using a computational approach, where, due to the presence of fluid pressure transients, the flow velocity field is both time- and space-dependent. The piezo-conduction equation is used in the study to determine the pore fluid pressure transients in a fluid-saturated porous medium. The time- and mesh-adaptive numerical schemes are proposed, respectively, for the modelling of one- and multi-dimensional advective transport problems with time- and space-dependent flow velocity to achieve an optimum computational performance. The computational results for one-dimensional semi-infinite domains as well as three-dimensional axisymmetric domains are presented to illustrate the need for adaptive procedures, for handling a non-classical hyperbolic conservation equation with time- and position-dependent advective flow velocities and with steep advective transport fronts.

REFERENCES

1. Bear J. *Dynamics of Fluids in Porous Media*. Dover Publications: New York, 1972.
2. Bear J, Verruijt A. *Modelling Groundwater Flow and Pollution*. D. Reidel Publ. Co.: Dordrecht, The Netherlands, 1990.
3. Bear J, Bachmat Y. *Introduction to Modelling of Transport Phenomena in Porous Media*. D. Reidel Publ. Co.: Dordrecht, The Netherlands, 1992.
4. Banks RB. *Growth and Diffusion Phenomena*: *Mathematical Frameworks and Applications*. Springer: Berlin, 1994.
5. Charbeneau R. *Groundwater Hydraulics*, *and Pollutant Transport*. Prentice-Hall: Upper Saddle River, NJ, 1999.
6. Selvadurai APS. *Partial Differential Equations in Mechanics*, vols. 1 and 2. Springer: Berlin, 2000.
7. Selvadurai APS. The advective transport of a chemical from a cavity in a porous medium. *Computers and Geotechnics* 2002; **29**:525–546.
8. Selvadurai APS. Contaminant migration from an axisymmetric source in a porous medium. *Water Resources Research* 2003; **39**(8):1204, WRR 001742.
9. Selvadurai APS. On the advective–diffusive transport in porous media in the presence of time-dependent velocities. *Geophysical Research Letters* 2004; **31**(13):L13505.
10. Selvadurai APS. Advective transport from a penny-shaped crack in a porous medium and an associated uniqueness theorem. *International Journal for Numerical and Analytical Methods in Geomechanics* 2004; **28**:191–208.
11. Biot MA. General theory of three-dimensional consolidation. *Journal of Applied Physics* 1941; **12**:155–164.
12. Lewis RW, Schrefler BA. *The Finite Element Method in the Static and Dynamic Deformation and Consolidation of Porous Media*. Wiley: New York, 1998.
13. Barenblatt GI, Entov VM, Ryzhik VM. *Theory of Fluid Flows Through Natural Rocks*. Kluwer Academic Publishers: Dordrecht, The Netherlands, 1990.
14. Selvadurai APS. Some remarks on the elastic drive equation. In *Environmental Geomechanics*, Vulliet L, Laloui L, Schrefler BA (eds). EPFL Press: Switzerland, 2002; 253–258.
15. Codina R. Comparison of some finite element methods for solving the diffusion–convection–reaction equation. *Computer Methods in Applied Mechanics and Engineering* 1998; **156**:185–210.
16. Wang Y, Hutter K. Comparisons of numerical methods with respect to convectively dominated problems. *International Journal for Numerical Methods in Fluids* 2001; **37**:721–745.
17. Hughes TJR, Brooks A. A theoretical framework for Petrov–Galerkin methods with discontinuous weighting functions: application to the streamline-upwind procedure. In *Finite Elements in Fluids*, Gallagher RH *et al*. (eds). Wiley: Chichester, U.K., 1982; 47–65.
18. Dong W, Selvadurai APS. Chemical transport in a fluid-saturated porous media. *Proceeding of the 9th Symposium on Numerical Models in Geomechanics—NUMOG IX*, Ottawa, Canada, 2004; 355–362.
19. Oñate E, García J, Idelsohn S. Computation of the stabilization parameter for the finite element solution of advective–diffusive problems. *International Journal for Numerical Methods in Fluids* 1997; **25**:1385–1407.
20. Carey GF, Jiang BN. Least squares finite element method and pre-conditioned conjugate gradient solution. *International Journal for Numerical Methods in Engineering* 1987; **24**:1283–1296.
21. Wendland E, Schmid GA. Symmetrical streamline stabilization scheme for high advective transport. *International Journal for Numerical and Analytical Methods in Geomechanics* 2000; **24**:29–45.
22. Raymond WH, Garder A. Selective damping in a Galerkin method for solving wave problems with variable grids. *Monthly Weather Review* 1976; **104**:1583–1590.

23. Donea J, Giulian S, Laval H, Quartapelle L. Time-accurate solution of advection–diffusion problem by finite elements. *Computer Methods in Applied Mechanics and Engineering* 1984; **45**:123–145.
24. Vichnevetsky R, Bowles JB. *Fourier Analysis of Numerical Approximations of Hyperbolic Equations*. SIAM: Philadelphia, PA, 1982.
25. Pereira JMC, Pereira JCF. Fourier analysis of several finite difference schemes for the one-dimensional unsteady convection–diffusion equation. *International Journal for Numerical Methods in Fluids* 2001; **36**:417–439.
26. Selvadurai APS, Dong W. A time-adaptive scheme for the accurate solution of the advective-transport equation with a transient flow velocity. *Computer Modeling in Engineering Science* 2006, in press.
27. Eriksson K, Johnson C. Adaptive finite element methods for parabolic problems. I: A linear model problem. *SIAM Journal on Numerical Analysis* 1991; **28**:43–77.
28. Carslaw H, Jaeger JC. *Heat Conduction in Solids*. Oxford University Press: Oxford, 1959.
29. Carey GF. Adaptive refinement and nonlinear fluid problems. *Computer Methods in Applied Mechanics and Engineering* 1979; **17/18**:541–560.
30. George PL. *Automatic Mesh Generation—Application to Finite Element Methods*. Wiley: Chichester, 1991.

